INTERNATIONAL JOURNAL OF AGRICULTURE & BIOLOGY
ISSN Print: 1560–8530; ISSN Online: 1814–9596
17–0609/2018/20–2–297–306
DOI: 10.17957/IJAB/15.0489
http://www.fspublishers.org

Full Length Article

HPLC-DAD-ESI-MS Fingerprinting and Antioxidant Potential of Phenolic Constituents Extracted from *Martynia annua*

Saba Muazzam and Muhammad Farman*
Department of Chemistry, Quaid-i-Azam University, Islamabad-45320, Pakistan
*For correspondence: farman@qau.edu.pk; saba_muazzam@yahoo.com

Abstract

Martynia annua Linn. (Family: Martyniceae), is a medicinally important plant being rich in phenolics. The current study was undertaken to investigate the phenolic acids and flavonoid glycosides using HPLC-DAD-ESI-MS fingerprinting and explore their total phenolic content (TPC), total flavonoid content (TFC) and antioxidant potential. Various parts of *M. annua* were extracted by ultrasound assisted solvent extraction and HPLC method was developed. Based on HPLC data, UV absorption and MS profiling, 23 compounds were putatively identified. Apigenin, luteolin, hispidulin and quercetin glycosides were the major flavonoid glycosides. Leaves and flower showed higher TPC (226.84 and 49.31 µg/mL respectively) and TFC (152.02 and 122.22 µg/mL respectively) and have promising antioxidant activity. So, it is demonstrated that, extracts from *M. annua* have high phenolic and flavonoid contents and antioxidant capacities. © 2018 Friends Science Publishers

Keywords: *Martynia annua*; Flavonoids; HPLC-DAD-ESI-MS; Antioxidants

Introduction

Martynia annua Linn. (Family Martyniaceae) is an annual plant found in Mexico, India and Pakistan. The species is known by various names such as cat's claw, devil's claw, bichchhu, pulinagam (Flora *et al*., 2013), kakanasika and vichchida (Nagda *et al*., 2009). Pharmacological studies revealed that, leaves have to be shown antiseptic activity, tuberculosis, inflammation and anti-convulsant activity (Babu *et al*., 2010; Dhingra *et al*., 2013). The leaf paste is used for the wounds of domestic animals and its juice is also applied as gargle for sore throat (Satyavati *et al*., 1987). The fruits are applied as a local sedative and also used as antidote to scorpion stings and venomous stings/bites (Watt, 1972).

Regarding its phytochemical composition, previously reported data on this species highlighted the presence of medicinally useful phyto constituents such as, tannins, alkaloids, glycosides, phenols, flavonoids and carbohydrates (Pillai *et al*., 1964; Parvati and Narayana, 1978). Flavonoids and phenolic acids are commonly regarded as the bioactive constituents of this species. Pelargonidin-3, 5-diglucoside and cyanidin-3-galactoside have been reported in flower whilst gentisic acid is present in fruits. The seeds show the presence of cyclopropenoid, linoleic acid, oleic acid, arachidic acid, palmitic acid, stearic acid and malvalic acid (Mali *et al*., 2002). The leaves contain apigenin, apigenin-7-*O*-glucuronide and luteolin (Lodhi and Singhai, 2013).

Polyphenolic compounds are the most important phytochemicals with various roles in plant defense system, demonstrate antioxidant activity and beneficial health effects. Polyphenolic compounds are used as major determinant of antioxidant potential and therefore are natural source of antioxidants. Besides other biological effects, the antioxidant activity, in particular, has gained the most interest and the biochemical properties of flavonoids are believed to come from their antioxidative properties (Scalbert *et al*., 2005).

In the last decade, important progress was made regarding extraction, identification and quantification of bioactive constituents, needed for the quality control of herbal formulation. Different analytical protocols have been established for the separation, identification and quantification of phenolic constituents in plant samples (Santos-Buelga and Williamson, 2003).

Recently, the concept of chromatographic fingerprinting analysis combined with spectroscopic detectors (*e.g.*, Diode Array Detector and Mass Spectrometry) has attained more popularity because it presents a more comprehensive profile of phenolic compounds. A serious issue concerning the plant extracts is low concentration of compounds that showed more potent bioactivity than those present in greater amount with lower activity. So, the screening of plant extracts for the presence of most active constituents, biological fingerprinting has been applied with the aid of High Performance Liquid Chromatography-Mass Spectrometry.

To cite this paper: Muazzam, S. and M. Farman, 2018. HPLC-DAD-ESI-MS fingerprinting and antioxidant potential of phenolic constituents extracted from *Martynia annua*. *Int. J. Agric. Biol*., 20: 297–306

These techniques have been reviewed by (Su *et al*., 2007; Yu *et al*., 2010; Ciesla, 2012). HPLC-DAD-ES1-MS technique has extensively been used for the fingerprinting analysis of phenolic constituents of plant extracts. The information gleaned from HPLC retention time, DAD and MS spectra helps in the identification of apt characterization of phenolic compounds (Quirantes *et al*., 2009).

So far, there are no reports on the polyphenolic profiling using analytical approaches and lack a detailed picture of antioxidant activity from this species. So in the context of current medicinal uses of this plant, the present investigation was aimed to characterize polyphenolic compounds using HPLC-DAD-ESI-MS analysis and to evaluate its total phenolic content, total flavonoid content and antioxidant activity.

Materials and Methods

Chemicals/Reagents

Analytical grade acetonitrile, formic acid, water, methanol and ethanol were procured from Merck (Darmstadt, Germany). Sodium carbonate, aluminum chloride, ferric chloride, sodium nitrite, sodium hydroxide, sodium acetate, Folin-Ciocalteu reagent, gallic acid, 2,4,6-tripyridyl-*s*-triazine (TPTZ), 1,1-diphenyl-2-picrylhdrazyl (DPPH), ferrous sulphate were purchased from Sigma-Aldrich (Gillingham, UK).

Plant Material

Aerial parts and roots of *M. annua* were collected in October–November 2013 from Quaid-i-Azam University, Islamabad campus. The plant was authenticated by a taxonomist, Dr. Zafar Iqbal, Department of Plant Sciences, Quaid-i-Azam University, Islamabad. A voucher specimen No. 308 was submitted in herbarium of the same department.

Extraction

For HPLC analysis: Whole plant (5 g) was shade-dried and pulverized. The powdery mass was extracted with methanol (25 mL) by employing ultrasound assisted extraction. After filtration, extract was evaporated to dryness under reduced pressure by rotary evaporator (BUCHI Rota vapor R-200) and resulting residue was dissolved in methanol for HPLC-MS analysis.

For Antioxidant activity: Each dried powdery mass (20 g) of plant parts (leaves, stem, fruits, flowers and roots) were dissolved in methanol (100 mL) and sonicated for 15 min in ultrasonic bath. Filtered the extracts through filter paper and evaporated under reduced pressure. The residues were dissolved in methanol for antioxidant activity.

Sample Preparation

The whole plant extract was prepared at 1 mg/mL concentration in methanol. The sample was diluted to 5 µg/mL and subjected to HPLC-MS analysis. For antioxidant activity, each plant part extracts were prepared at the same concentration in methanol *i.e.*, 1 mg/mL and further diluted to different concentration with methanol.

HPLC-DAD-ESI-MS Analysis

HPLC analysis was performed using Agilents 1200 series liquid chromatography system coupled with Chem Station for LC. 3D system Rev. B01.03 [2004] equipped with quaternary pump (GI311A), auto sampler (GI329A), degasser (GI322A), and thermos column compartment (G3I6A). For LC separation of extracts, a Waters symmetry HPLC stainless steel column (4.6×150 mm) packed with 5 µm Agilent Eclipse XDB C-18. Column temperature maintained at 35ºC. Mobile phase composition was as follows; Solvent A (Water containing 0.1% formic acid) and Solvent B (Acetonitrile). The run time was set to 60 min. with linear gradient change from solvent B; 10% at 0–15 min, 10–40% at 15–40 min, 40–80% at 40–50 min and 10% at 60 min. Sample injection volume was 5 µL and flow rate was set at 0.5 mL/min. DAD spectra were acquired at 254, 320 and 370 nm.

Mas spectrometric analysis was performed using Agilents mass detector MS 6310 (Ion trap LC/MS) equipped with an electrospray ionization (ESI). Operating parameters were as follows; positive ionization mode, capillary voltage -3.5 kV, source voltage (1nA), capillary temperature (325ºC), sheath gas, nitrogen generator N-118LA, Edward EIM18 pump (A22304199). Experiment was operated in fu1l scan mode (0-1000 *amu*).

Estimation of Total Phenolic Contents (TPC)

The total phenolic content was determined by Folin-Ciocalteu reagent assay (Singleton *et al*., 1999). Aliquots of 100 mg lyophilized powder of plant material were dissolved in 1 mL of MeOH. Mixed this 0.1 mL of plant extract with 2.8 mL deionized water, 0.1 mL of 50% Folin-Ciocalteu reagent and 2 mL of 2% sodium bicarbonate and reaction mixture was incubated for 30 min at room temperature. Absorbance was recorded at 750 nm on a Cary 4000 UV-Vis spectrophotometer. Total phenolic contents were expressed as µg/mL GAE using the seven point standard curve of gallic acid.

Estimation of Total Flavonoid Contents (TFC)

The total flavonoid content was measured by aluminum chloride colorimetric assay (Chang *et al*., 2002). Aliquots of 100 mg plant material were dissolved in 1 mL MeOH. To this 0.5 mL of extract, add 1.5 mL of alcohol (95%), 0.1 mL aluminum chloride (10%), 2.8 mL deionized water and 0.1 mL potassium acetate (1 M).

Incubation of reaction mixture was performed for 40 min at room temperature and absorbance was recorded at 415 nm. Total flavonoid contents were measured by standard calibration curve constructed for Rutin and expressed as µg/mL RE.

DPPH Antioxidant Assay

Antioxidant activity of plant extracts were determined by DPPH assay (Brand-William *et al*., 1995). One mL of plant extract at different concentration (400, 200, 100 and 50 µg/mL) was mixed with 3 mL of 0.1 mM DPPH solution in methanol. Mixture was allowed to stand at room temperature for 30 min and absorbance was taken at 517 nm.

Antioxidant potential was expressed in term of percentage inhibition and IC_{50} values with reference compound Gallic acid. Percentage inhibition was calculated using following equation:

$$(\%)\text{ age inhibition} = A_{control}\text{-}A_{sample}/A_{control} \times 100$$

ABTS Antioxidant Method

Polyphenolic compounds have the ability to scavenge $ABTS^{\cdot+}$ radical cation and this was produced by reaction of ABTS stock solution (7 mM) and potassium persulfate (2.5 mM) in 1:1 (v/v). The mixture was kept overnight and then diluted to 0.700 ± 0.500 at 734 nm with MeOH. One mL of the extracts at different concentrations (400, 200, 100 and 50 µg/mL) was added to 4 mL $ABTS^{\cdot+}$ solution and absorbance was recorded immediately at 734 nm. Percentage inhibition and IC_{50} values were calculated with the reference compound Trolox (Arnao *et al*., 2001).

FRAP Reducing Antioxidant Method

The reducing ability of polyphenolic compounds were measured by FRAP method (Benzie and Strain, 1996). The fresh working reagent was prepared by dissolving 300 mM sodium acetate buffer (pH 3.6), 20 mM $FeCl_3.6H_2O$ and 10 mM 2,4,6-tripyridyl-*s*-triazine (TPTZ) in 40 mM hydrochloric acid in proportion of 10:1:1 (v/v/v). Then 4 mL of this FRAP reagent was mixed with 1 mL of plant extracts and incubated for 30 min at 37ºC. A change in color was observed and absorbance was measured at 593 nm. Antioxidant capacity was calculated from the linear calibration curve of $FeSO_4$ and expressed in µM Fe^{2+}/g.

Statistical Analysis

Each experiment was performed in triplicate. Analysis of variance under CRD was used to test any difference in antioxidant activities resulting from different methods. Equations for best fitted line to estimate IC_{50} and correlation coefficient values obtained by using linear regression analysis were used to fit a line to a set of experimental results using the "least squares". Data were analyzed using Microsoft Excel 2010, GraphPad Prism 7 and Statistics 8.1.

Results

Phenolic acids and flavonoid glycosides from the extract of *M. annua* were separated by HPLC coupled to both DAD and MS detectors. The HPLC chromatogram (Fig. 1) registered at three different wavelengths 254, 320 and 370 nm because the different classes of phenolic compounds exhibit absorption maxima at different wavelengths.

A total of 23 compounds including four phenolic acid derivatives and 19 flavonoids including methylated and acylated flavone and flavonol glycosides have been tentatively characterized (Table 1). The structures of these compounds (Fig. 2) were suggested using the established methods of interpreting these data.

Identification of Phenolic Acid Glycosides

Phenolic acids appeared earlier in the HPLC chromatogram where eluent composition is changed *i.e.,* 10% of acetonitrile (Solvent B) which suggested the hydrophilic character of the eluting compounds that indicating the phenolic acid or ester family. The UV spectra revealed that the compounds 1, 2 and 3 have benzoic acid skeleton and 4 have chlorogenic acid core structure. When the phenolic derivatives exhibited bathochromic shifts (shifts to longer wavelength), this suggested the esterification of the aglycone with sugars, and when they showed hypsochromic shifts (to shorter wavelength) this indicated glycosylation.

The MS spectrum of compound 1 indicated peak at *m/z* 932 $[M+H_2O+2H]^+$.The molar mass of the compound is 912 *amu* $[M]^+$. The fragment ion peaks appeared at *m/z* 793 $[M+H\text{-}^{0,2}X_{0glc}]^+$ by the loss of $^{0,2}X_0$ fragment of glucose moiety. The peak at *m/z* 585 $[M+K\text{-diglc-acetyl}]^+$ was attributed to the loss of diglucoside moieties along with acetyl molecule. Peak at *m/z* 285 was inferred by the loss of 650 mass units due to the cleavage of diacetyl rhamnose moiety, acetyl diglucoside residues along with three water molecules *i.e.,* $[M+Na\text{-rha-diacetyl-diglc-acetyl-}3H_2O]^+$. RT, UV data, and diagnostic MS fragments suggested the compound as *p*-hydroxy-4-*O*-(β-*D*-glucosyl (1→4)- (2',3'-diacetyl)-α-*L*-rhamnosyl-(1→4)-β-*D*-glucosyl-(1→4)- (2'-acetyl)- β-*D*-glucoside) benzoic acid.

Compound 2 have major signal ion peak at *m/z* 905 $[M+Na]^+$. So, molar mass of the compound is 882 *amu* $[M]^+$. The characteristic fragments ions viewed at *m/z* 823 $[M+H\text{-}^{0,3}X_3xyl]^+$ by the loss of $^{0,3}X$ fragment of xylose. Peak at *m/z* 623 was inferred by the loss of acetylxylosyl moiety, $^{0,3}X$ fragment of glucose moiety along with one H_2O molecule *i.e.,* $[M+Na\text{-acetylxyl-}^{0,3}X_2glc\text{-}H_2O]^+$. The fragment peak appeared at *m/z* 343due to the loss of acetylxyloside moiety, one glucose moiety and acetylglucoside moiety *i.e.,*$[M+CH_3CN+2H\text{-acetylxyl-glc-acetylglc}]^+$. These results suggested the compound as *p*-hydroxy-4-*O*-(β-*D*-glucosyl-(1→4)-(2',6'-diacetyl)- β-*D*-glucosyl-(1→4)-β-*D*-xyloside) benzoic acid.

Table 1: The UV absorption data and MS fragmentation (positive ion mode) of phenolic acids and flavonoid glycosides identified from *M. annua*

No.	RT (min.)	UV λ_{max} (nm)	ESI-MS	Fragments ions (*m/z*)	Identification
1	3.1	260	889[M+H_2O+H]$^+$	793,**585**,495,318,285, 231,174	*p*-hydroxy-4-*O*-(β-*D*-glucosyl (1→4)- (2',3'-diacetyl)- α-*L*-rhamnosyl-(1→4)-β-*D*-glucosyl-(1→4)- (2'-acetyl)- β-*D*-glucoside) benzoic acid
2	3.4	254	905 [M+Na]$^+$	823,713,663,585,397, **343**,275	*p*-hydroxy-4-*O*-(β-*D*-glucosyl-(1→4)-(2',6'-diacetyl)- β-*D*-glucosyl-(1→4)-β-*D*- xyloside) benzoic acid
3	10.8	260	871[M+H]$^+$	623,565,**517**,473,411, 377	3,4-dihydroxy-4′-*O* [(2',6'-diacetyl)-β-*D*-glucosyl-(1→4)-α-*L*-rhamnosyl-(1→4)- β-*D*-glucosyl -(1→4)-β-*D*-glucoside] benzoic acid
4	23.9	244,300sh,327	663[M+H]$^+$	**663**	3(3,4-dihydroxycinnamoyl-[3'-*O* (β-*D*-glucosyl-(1→4) α-*L*-rhamnoside)] quinic acid
5	25.5	228,307	850[M+CH_3CN+H]$^+$	755,705,**563**,497,439, 413,285	4′-methoxy-5,7-dihydroxyflavone-7-*O*-(β-*D*-xylosyl-(1→4)- α-*L*-rhamnosyl-(1→4)-(2",3"-diacetyl)-β-*D*- glucoside)
6	27.2	286,324	661[M+K]$^+$, 623[M+H]$^+$	**661**,471,403,325	3′,4′,5′-trihydroxy-5,7-dihydroxyflavone-7-*O*-(α-*L*-rhamnosyl-(1→4)-(2" acetyl)-β-*D*-xyloside)
7	29.4	343,255,270sh	647[M+$2H_2O$+H]$^+$	563,**463**,325,287	Luteolin-7-*O*-(β-*D*-glucosyl-(1→4)-β-*D*-glucoside)
8	29.7	248sh,266,288sh,341	788[M+2H]$^{2+}$	647,**463**,287	Luteolin-7-*O*-(β-*D*-glucuronide-(1→4)-β-*D*-glucoside)
9	30.1	252,278,288,330	717[M+K]$^+$	**717**,627,463,301	Hispidulin-7-*O*-(β-*D*-glucosyl-(1→4)- (2',3'-diacetyl)- β-*D*-xyloside)
10	31.0	329,247,287sh	691[M+CH_3OH+H]$^+$	647,569,517,463,437, 415,**273**	3′,4′-dihydroxyflavone-4′-*O*-(α-*L*-rhamnosyl-(1→4)-β-*D*-glucosyl(1→4) -β-*D*-glucoside)
11	32.5	266,336	893[2M+H]$^+$	**447**,271	Apigenin-7-*O*-(β-*D*-glucuronide) Dimer
12	32.6	335,368	931[M+CH_3OH+H]$^+$	851,806,525,**447**,389, 271	Apigenin-7-*O*-(β-*D*-glucosyl-(1→4)-α-*L*-rhamnosyl-(1→4)-α-*L*-rhamnosyl-(1→4)-(2"-acetyl)- β-*D*-xyloside)
13	33.1	251,265sh,340	953[2M+H]$^+$	**477**,301	Hispidulin-7-*O*-(β-*D*-glucuronide) Dimer
14	38.2	251,266sh.290sh,346	897[M+Na]$^+$	707,593,**287**	Luteolin-7-*O*-(β-*D*-glucosyl-(1→4)-β-*D*-glucosyl-(1→4)- β-*D*-xylosyl-(1→4)-β-*D*-xyloside)
15	38.4	368,247	611 [M+H]$^+$	551,507,469,389,331, **207**	Quercetin-3-*O*-(β-*D*-glucosyl-(1→4)-α-*L*-rhamnoside) (Rutin)
16	41.5	322,238,296sh	833[M+$3H_2O$+H]$^+$	749,**674**,609,441,498, 255	3′,4′-dihydroxyflavone-4′-*O*-[(2"'-acetyl)- β-*D*-xylosyl-(1→4)-(2"-acetyl)-β-*D*-glucosy-(1→4)- α-*L*-rhamnoside]
17	42.2	267,290sh,336	849[M+Na]$^+$	785,691,563,313,**271**	Apigenin-7-*O*-(α-*L*-rhamnosyl)-(1→4)- α-*L*-rhamnosyl-(1→4)-β-*D*-xylosyl-(1→4)-β-*D*-xyloside)
18	42.3	335,268,301sh	960[M+H_2O+2H]$^+$	873,829,785,741,695, 653,565, 513,441,389,**351**	Apigenin-4′-*O*-(α-*L*-rhamnosyl-(1→4)-(2″-acetyl)-α-*L*-rhamnosyl-(1→4)-β-*D*-glucosyl-(1→4)-(2"'-acetyl)-β-*D*-xyloside)
19	42.7	248sh,268sh,350	965[M+H]$^+$	875,683,633,543,447, **331**	3′,5′-dimethoxy-4′,5,7-trihydroxyflavone-7-*O*-[(2″-acetyl)-β-*D*-xylosyl-(1→4)-α-*L*-rhamnosyl-(1→4)-(2-galloyl)-β-*D*-glucoside]
20	43.2	250,266sh, 290,347	755[M+H]$^+$	613,447,369,**301**	Hispidulin-7-*O*-(α-*L*-rhamnosyl-(1→4)-β-*D*-glucosyl-(1→4)- α-*L*-rhamnoside
21	44.2	370,250	843[M+H]$^+$	799,755,711,667,579, 535,**447**,389,345	Quercetin-3-*O*-(β-*D*-glucosyl-(1→4)-(6"-acetyl)- β-*D*-glucosyl-(1→4)-(2"'-acetyl)-β-*D*-xyloside)
22	49.9	310,236,275sh	959[M+CH_3OH+H]$^+$	797,719,637,583,549, 505,469,371,**313**	3′,4′-dimethoxy-7-hydroxyflavone-7-*O*-[(2″-acetyl)-β-*D*-xylosyl-(1→4)-α-*L*-rhamnosyl-(1→4)-α-*L*-rhamnosyl-(1→4)-β-*D*-glucoside]
23	55.7	327,271	971[M+CH_3CN+2H]$^+$	719,671,627,592,539, 497,415,325,**303**	4′-methoxy-5,7-dihydroxyflavone-7-*O*-(β-*D*- glucosyl-(1→4)- β-*D*-glucosyl-(1→4)-β-*D*- xylosyl-(1→4)-(2"'-acetyl)-α-*L*-rhamnoside)

Values in bold indicating base peak

Compound 3 gave signal at *m/z* 871 [M+H]$^+$. The molecular mass of the compound is 870 [M]$^+$. MS fragments appeared at *m/z* 623 due to the loss of one glucose moiety, ^{0,3}X fragment of glucoside moiety along with one water molecule *i.e.,* [M+Na-glc-$^{0,3}X_{2glc}$-H_2O]. The high intensity signal referred to as base peak appeared at *m/z* 517by the loss of diglucoside moieties along with one molecule of formaldehyde and water *i.e.,* [M+H_2O+H-diglc-CH_2O-H_2O]$^+$. On the basis of these results compound was deduced as 3,4-dihydroxy-4′-*O* [(2',6'-diacetyl)-β-*D*-glucosyl-(1→4)-α-*L*-rhamnosyl-(1→4)- β-*D*-glucosyl-(1→4)-β-*D*-glucoside] benzoic acid.

Compound 4 showed in the mass spectrum at *m/z* 663 [M+H]$^+$ and molecular mass is 662 [M]$^+$. A loss of 308 mass units from the molecular mass gave the indication of chlorogenic acid as a core skeleton (*m/z* 354) and indicated the attachment of hexose and rhamnose moieties. Hypsochromic shift of 27 nm suggested the glycosylation of –OH group of caffeic acid moiety. The results identified the compound as chlorgenic acid rutinoside.

Identification of Flavonoid Glycosides

Flavonoid glycosides appeared in the middle region of HPLC chromatogram where eluent composition is changed to 10–40% with solvent B, highlighting the hydrophilic nature of the eluting compound and gave the indication of flavonoid moiety.

Compound 5 and 23 identified as 4′-methoxy-5, 7-dihydroxyflavone derivatives with substitution at position 7. Compound 5 showed signal at *m/z* 850 [M+CH_3CN+H]$^+$ with the molar mass of compound is 808 [M]$^+$. Major diagnostic fragments ions appeared at *m/z* 705 [M+Na-$^{0,3}X_2$glc-2H_2O]$^+$, *m/z* 563[M+H-glc-diacetyl]$^+$, *m/z* 497 [M+K-glc-diacetyl-$^{0,2}X_1$rha]$^+$ and aglycone peak at *m/z* 285 [Agl+H]$^+$. On the basis of these results the compound suggested as 4′-methoxy-5, 7-dihydroxyflavone-7-*O*-(β-*D*-xylosyl-(1→4)- α-*L*-rhamnosyl-(1→4)-(2",3"-diacetyl)-β-*D*- glucoside). Compound 23 gave signal at *m/z* 971 [M+CH_3CN+2H]$^+$ with molecular mass 928 [M]$^+$.

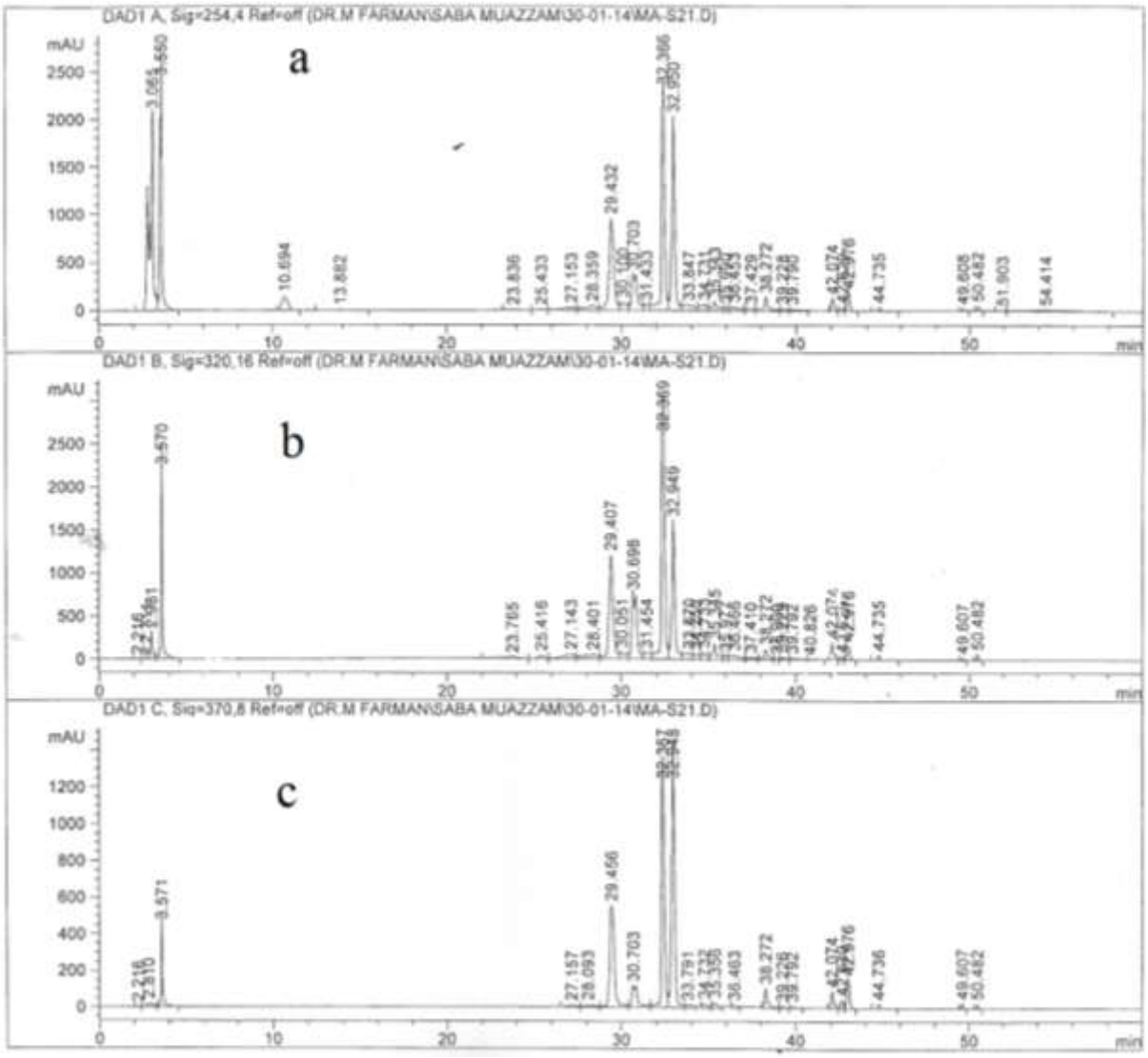

Fig. 1: HPLC chromatogram of methanolic extract of *M. annua* at three different wavelengths **(a)** 254 nm **(b)** 320 nm and **(c)** 370 nm

Fragments ion appeared at *m/z* 719 [M+K-acetylrha-$^{0,3}X_2$xyl]$^+$, *m/z* 627 ,[M+H_2O+H-acetylrha-xyl]$^+$, *m/z* 539 [M+K-acetylrha-xyl-$^{0,3}X_1$glc-H_2O]$^+$ and *m/z* 303[282+H_2O+H]$^+$ .These data identified the compound as 4′-methoxy-5,7-dihydroxyflavone-7-*O*-(β-*D*- glucosyl-(1→4)- β-*D*-glucosyl-(1→4)-β-*D*- xylosyl-(1→4)-(2‴-acetyl)-α-*L*-rhamnoside).

Compound 6 identified as penta hydroxylated acetylated flavone glycoside. Major ions peak appeared at *m/z* 623 [M+H]$^+$ and *m/z*661 [M+K]$^+$ with two different adducts. Further diagnostic fragments appeared at *m/z* 471 [M+Na-acetylxyl]$^+$ and *m/z* 325 [302+Na]$^+$. The compound was identified as 3′,4′,5′-trihydroxy-5,7-dihydroxyflavone-7-*O*-(α-*L*-rhamnosyl-(1→4)-(2" acetyl)-β-*D*-xyloside).

The UV spectra and mass fragmentation data of compound 7, 8 and 14 supported the identity of Luteolin as aglycone moiety with the glycosylation at positions 7. Compound 7 represent major signal at *m/z* 647 [M+2H_2O+H]$^+$ and further diagnostic signals at *m/z* 563 [M+CH_3CN+2H-$^{0,3}X_{1glc}$]$^+$, *m/z* 463 [M+CH_3OH+H-glc-H_2O]$^+$. Aglycone peak at *m/z* 287 [286+H]$^+$ inferred the core skeleton as luteolin. These results suggested the compound as Luteolin-7-*O*-(β-*D*-glucosyl-(1→4)-β-*D*-glucoside). Compound 8 showed pseudomolecular ion peak at *m/z* 788 [M+2H]$^{2+}$. Further fragments appeared at *m/z* 647 [M+Na-glc]$^+$, *m/z* 463[M+CH_3OH+H-glc-glucuronide-H_2O]$^+$, aglycone peak at *m/z* 287 [286+H]$^+$ and the compound was identified as Luteolin-7-*O*-(β-*D*-glucuronide-(1→4)-β-*D*-glucoside). Compound 14 represents pseudomolecular ion peak at 897 [M+Na]$^+$ with fragments ion peak at *m/z* 707 [M+H-xyl-2H_2O]$^+$,*m/z* 593 [M+H-dixyl-H_2O]$^+$, *m/z* 287 [286+H]$^+$ Luteolin-7-*O*-(β-*D*-

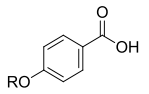

1 R=(β-*D*-glucosyl (1→4)- (2',3'-diacetyl)- α-*L*-rhamnosyl-(1→4)-β-*D*-glucosyl-(1→4)- (2'-acetyl)- β-*D*-glucoside)
2 R= (β-*D*-glucosyl-(1→4)-(2',6'-diacetyl)- β-*D*-glucosyl-(1→4)-β-*D*- xyloside)

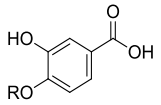

3 R= [(2',6'-diacetyl)-β-*D*-glucosyl-(1→4)-α-*L*-rhamnosyl-(1→4)- β-*D*-glucosyl -(1→4)-β-*D*-glucoside]

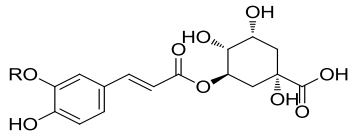

4 R= 3´-*O* (β-*D*-glucosyl-(1→4) α-*L*-rhamnoside)

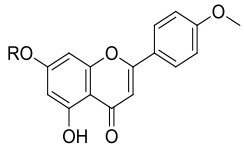

5 R= 7-*O*-(-β-*D*-xylosyl-(1→4)- α-*L*-rhamnosyl-(1→4)-(2",3"-diacetyl)-β-*D*- glucoside)
23 R= 7-*O*-(β-*D*- glucosyl-(1→4)- β-*D*-glucosyl-(1→4)-β-*D*- xylosyl-(1→4)-(2‴-acetyl)-α-*L*-rhamnoside)

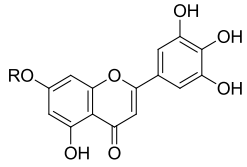

6 R= 7-*O*-(α-*L*-rhamnosyl-(1→4)-(2" acetyl)-β-*D*-xyloside)

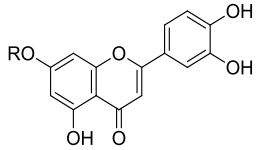

7 R= 7-*O*-(β-*D*-glucosyl-(1→4)-β-*D*-glucoside)
8 R= 7-*O*-(β-*D*-glucuronide-(1→4)-β-*D*-glucoside)
14 R= 7-*O*-(β-*D*-glucosyl-(1→4)- β-*D*-glucosyl-(1→4)- β-*D*-xylosyl-(1→4)- β-*D*-xyloside)

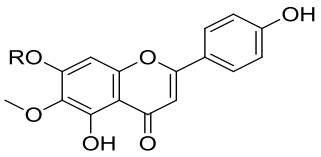

9 R= 7-*O*-(β-*D*-glucosyl-(1→4)- (2',3'-diacetyl)- β-*D*-xyloside)
13 R= 7-*O*-(β-*D*-glucuronide)
20 R= 7-*O*-(α-*L*-rhamnosyl-(1→4)-β-*D*-glucosyl-(1→4)- α-*L*-rhamnoside)

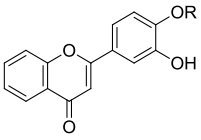

10 R= 4′-*O*-(α-*L*-rhamnosyl-(1→4)-β-*D*-glucosyl(1→4) -β-*D*-glucoside)
16 R= 4′-*O*-[(2"'-acetyl)- β-*D*-xylosyl-(1→4)-(2"-acetyl)-β-*D*-glucosy-(1→4)- α-*L*- rhamnoside]

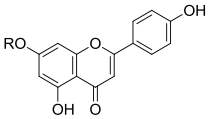

11 R=7-*O*-(β-*D*-glucuronide)
12 R= 7-*O*-(β-*D*-glucosyl-(1→4)-α-*L*-rhamnosyl-(1→4)-α-*L*-rhamnosyl-(1→4)- (2"-acetyl)- β-*D*-xyloside)
17 R= 7-*O*-(α-*L*-rhamnosyl)- (1→4)- α-*L*-rhamnosyl-(1→4)-β-*D*-xylosyl-(1→4)-β-*D*-xyloside)
18 R=4′-*O*-(α-*L*-rhamnosyl-(1→4)-(2"-acetyl)-α-*L*-rhamnosyl-(1→4)-β-*D*-glucosyl-(1→4)-(2"'-acetyl)-β-*D*-xyloside)

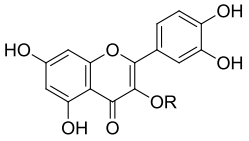

15 R= 3-*O*-(β-*D*-glucosyl-(1→4)-α-*L*-rhamnoside)
21 R= 3-*O*-(β-*D*-glucosyl-(1→4)-(6"-acetyl)- β-*D*-glucosyl-(1→4)-(2"'-acetyl)-β-*D*-xyloside)

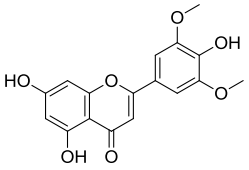

19 R= 7-*O*-[(2″-acetyl)-β-*D*-xylosyl-(1→4)- α-L-rhamnosyl-(1→4)-(2-galloyl)-β-*D*-glucoside]

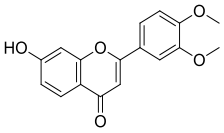

22 R= 7-*O*-[(2″-acetyl)-β-*D*-xylosyl-(1→4)-α-*L*-rhamnosyl-(1→4)-α-*L*-rhamnosyl-(1→4)-β-*D*-glucoside]

Fig. 2: Structures of phenolic acids and flavonoid glycosides identified from *M. annua*

glucosyl-(1→4)-β-*D*-glucosyl-(1→4)- β-*D*-xylosyl-(1→4)-β-*D*-xyloside) was proposed for the compound 14.

Compound 9, 13 and 20 were identified as hispidulin derivatives. UV absorption and shapes of bands support the identification of hispidulin as aglycone part. Pseudomolecular ion peak of Compound 9 appeared in the MS spectrum at *m/z* 717 $[M+K]^+$. Fragment ions signals appeared at *m/z* 627 $[M+CH_3OH$-diacetyl$]^+$, *m/z* 463 [M+Hxyl-diacetyl]$^+$. The aglycone signal appeared at *m/z* 301 $[Agl+H]^+$. On these results compound was inferred as Hispidulin-7-*O*-(β-*D*-glucosyl-(1→4)-(2',3'-diacetyl)-β-*D*-xyloside). Compound 13 represent pseudomolecular ion signal at *m/z* 953 $[2M+H]^+$ indicated a dimer of hispidulin-7-*O*-β-*D*-glucuronide. Two major fragments appeared at *m/z* 463 $[300+176+H]^+$ and aglycone peak appeared at *m/z* 301 $[Agl+H]^+$.

The data suggested the compound as Hispidulin-7-*O*-(β-*D*-glucuronide). The peak of Compound 20 showed at *m/z* 755 $[M+H]^+$ with major diagnostic peaks at *m/z* 613 $[M+Na\text{-}rha\text{-}H_2O]^+$, *m/z* 447 $[M+H\text{-}glc\text{-}rha]^+$ and *m/z* 301 $[M+H]^+$ and these results proposed the compound as Hispidulin-7-*O*-(α-*L*-rhamnosyl-(1→4)-β-*D*-glucosyl-(1→4)-α-*L*-rhamnoside.

The UV spectra revealed the Compound 10 and 16 as the derivatives of 3′,4′-dihydroxyflavone. In the MS spectrum of Compound 10 pseudomolecular ion signal appeared at *m/z* 691$[M+CH_3OH+H]^+$. Further fragment ions peaks showed at *m/z* 647 $[M+CH_3CN+2H\text{-}^{0,3}X_2glc\text{-}CH_2O]^+$, *m/z* 463 $[M+K\text{-}glc\text{-}^{0,3}X_1glc\text{-}CH_2O\text{-}H_2O]^+$, *m/z* 273 $[254+H_2O+H]^+$ and the structure of this compound deduced

as 3′,4′-dihydroxyflavone-4′-*O*-(α-*L*-rhamnosyl-(1→4)-β-*D*-glucosyl(1→4) -β-*D*-glucoside). Compound 16 represent molecular signal at *m/z* 833 $[M+3H_2O+H]^+$. Fragments ions peak appeared at *m/z* 674 $[M+CH_3OH+H\text{-rha}]^+$ and *m/z* 498 $[M+CH_3CN+H\text{-rha-acety}^{l,5}X_1glc]^+$. Peak at *m/z* 255 $[Agl+H]^+$ inferred the aglycone structure. On the basis of these results compound was identified as 3′,4′-dihydroxyflavone-4′-*O*-[(2"'-acetyl)- β-*D*-xylosyl-(1→4)-(2"-acetyl)-β-*D*-glucosy-(1→4)- α-*L*-rhamnoside].

The UV spectra of compounds 11, 12 and 17 which were identical, suggested that they were 7-*O*-glycosides of apigenin. Compound 18 identified as the 4´-*O*-glycosides of Apigenin. Compound 11 indicated pseudomolecular ion peak at *m/z* 893 $[2M+H]^+$. Two diagnostic fragments appeared at *m/z*447 [270+glucuronide (176)+H]$^+$ and aglycone (Apigenin) peak at *m/z* 271 $[Agl+H]^+$ suggested the compound as Apigenin-7-*O*-(β-*D*-glucuronide) dimer. Compound 12 showed molecular ion signal at *m/z* 931 $[M+CH_3OH+H]^+$. Fragments peaks appeared at *m/z* 851 $[M+CH_3CN+2H\text{-}^{0,2}X_{3xyl}]^+$, *m/z* 661 $[M+CH_3CN\text{-acetylxyl-}^{0,3}X_{2rha}\text{-}CH_2O]^+$,*m/z* 447 $[M+CH_3OH+H\text{-acetylxyl-dirha-}H_2O]^+$ and aglycone peak appeared at *m/z* 271 $[Agl+H]^+$. These fragmentation identified this compound as Apigenin-7-*O*-(β-*D*-glucosyl-(1→4)-α-*L*-rhamnosyl-(1→4)-α-*L*-rhamnosyl-(1→4)- (2"-acetyl)- β-*D*-xyloside). Pseudomolecular ion peak of compound 17 appeared in the MS spectrum at *m/z* 849 $[M+Na]^+$. Major fragments appeared at *m/z* 785 $[M+H_2O+H\text{-}^{0,3}X_{3xyl}]^+$, *m/z* 691 $[M+CH_3OH+H\text{-xyl-}H_2O]^+$ *m/z* 563 $[M+H\text{-dixyl}]^+$. Aglycone peak at *m/z* 271 $[270+H]^+$ and the structure was proposed as Apigenin-7-*O*-(α-*L*-rhamnosyl)-(1→4)-α-*L*-rhamnosyl-(1→4)-β-*D*-xylosyl-(1→4)-β-*D*-xyloside).

Compound 18 showed pseudomolecular ion peak at *m/z* 960 $[M+H_2O+2H]^+$ with major fragments peak at *m/z* 829 $[M+Na\text{-}^{1,5}X_3xyl\text{-}CH_2O]^+$, *m/z* 741 $[M+Na\text{-acetylxyl-}CH_2O\text{-}H_2O]^+$, *m/z* 565 $[M+K\text{-acetylxyl-glc-}2CH_2O\text{-}H_2O]^+$, *m/z* 389 $[M+K\text{-acetylxyl-glc-acetylrha-}CH_2O\text{-}2H_2O]^+$ and *m/z* 351 $[M+K\text{-acetylxyl-glc-acetylrha-}^{0,3}X_0rha\text{-}CH_2O]^+$. This compound was proposed as Apigenin-4′-*O*-(α-*L*-rhamnosyl-(1→4)-(2″-acetyl)-α-*L*-rhamnosyl-(1→4)-β-*D*-glucosyl-(1→4)-(2"'-acetyl)-β-*D*-xyloside).

The UV spectra are in agreement with the identification of Compound 15 and 21 as quercetin derivatives. The band I absorbs at longer wavelength *i.e.,* greater than 350 nm suggesting the aglycone as flavonol. Compound 15 appeared pseudomolecular ion peak at *m/z* 611 $[M+H]^+$ and this is characteristic of Rutin a well-known flavonoid. Further fragments appeared at *m/z* 507 $[M+H\text{-}^{0,2}X_1rha]^+$, *m/z* 469$[M+Na\text{-rha-}H_2O]^+$, *m/z* 331$[M+H\text{-rha-}^{1,5}X_0glc\ ]^+$ and *m/z* 303 $[M+H]^+$. Pseudomolecular ion peak of Compound 21 appeared at *m/z* 843$[M+H]^+$. Fragments ion peaks appeared at *m/z* 755 $[M+CH_3OH+H\text{-}^{0,3}X_2xyl\text{-acetyl-}H_2O]^+$, *m/z* 579 $[M+H\text{-acetylxyl-}^{0,3}X_1glc]^+$,*m/z* 535 $[M+Na\text{-acetylxyl-}^{0,2}X_1glc\text{-}2H_2O]^+$ and *m/z* 447 $[M+H_2O+H\text{-acetylxyl-acetylglc-}2H_2O]^+$. These data suggested the compound as Quercetin-3-*O*-(β-*D*-glucosyl-(1→4)-(6"-acetyl)- β-*D*-glucosyl-(1→4)-(2‴-acetyl)-β-*D*-xyloside).

Compound 19 and 22 identified as methoxyflavone glycosides. Pseudomolecular ion peak of compound 19 appeared in MS spectrum at *m/z* 965 $[M+H]^+$. Major fragments peak appeared at *m/z* 683 $[M+CH_3OH+H\text{-galloylglc}]^+$, *m/z* 543[M+K-galloylglc-rha]$^+$, *m/z* 447 $[M+ CH_3OH+H\text{-galloylglc-rha-}^{0,2}X_0xyl]^+$ and *m/z* 331 $[M+H]^+$ and Compound 22 showed molecular ion signal at *m/z* 959 $[M+CH_3OH+H]^+$. Further fragment peaks appeared at *m/z* 797 $[M+CH_3OH+H\text{-glc}]^+$, *m/z* 637 $[M+H_2O+H\text{-glc-rha}]^+$, *m/z* 583 $[M+K\text{-glc-rha-}^{0,3}X_1rha]^+$, *m/z* 505 $[M+CH_3OH+H\text{-glc-dirha}]^+$, *m/z* 371 $[M+H_2O+H\text{-glc-dirha-}^{0,2}X_0xyl\text{-}CH_2O]^+$ and *m/z* 313 $[M+Na\text{-glc-dirha-acetyl-}^{1,5}X_0xyl\text{-}2H_2O]^+$. These results suggested the compound 19 and 22 could be3′,5′-dimethoxy-4′,5,7-trihydroxyflavone-7-*O*-[(2″-acetyl)-β-*D*-xylosyl-(1→4)-α-*L*-rhamnosyl-(1→4)-(2-galloyl)-β-*D*-glucoside](19) and 3′,4′-dimethoxy-7-hydroxyflavone-7-*O*-[(2″-acetyl)-β-*D*-xylosyl-(1→4)-α-*L*-rhamnosyl-(1→4)-α-*L*-rhamnosyl-(1→4)-β-*D*-glucoside] (22).

Total Phenolic Content

The present study revealed the phenolic content of leaves, stem, fruits, flowers and roots of *M. annua*. The values obtained for total phenolic contents were expressed as µg/mL gallic acid equivalent (GAE) (Table 2). The phenolic content was calculated by using calibration equation y= 0.0011x+0.0163, where the coefficient of determination (R^2) value is 0.99.

The methanol extract of leaves have found to contain considerable amount of phenolic content *i.e.,* 226.84 µg/mL whilst stem has lowest *i.e.,* 56.79 µg/mL gallic acid equivalents. The order of TPC among different parts of the plant is as follows: Leaves > Flowers > Roots > Fruit > Stem. These results showed that the leaves and flowers are quite rich in phenolic compounds.

Total Flavonoid Content

TFC of plant extracts was analyzed using a standard calibration curve of Rutin. The flavonoid contents were expressed in µg/mL rutin equivalent (RE) (Table 2). TFC was calculated by using calibration equation y= 0.0009x-0.017 where the coefficient of determination (R^2) value is 0.98. Leaves and flowers contained higher flavonoids content *i.e.,* (152.02 and 122.22 µg/mL), respectively. The lowest amount of flavonoid content was found in Stem *i.e.,* 21.78 µg/mL. The order of TFC was same as TPC *i.e.,* Leaves > Flowers > Roots > Fruit > Stem.

DPPH Antioxidant Activity

DPPH antioxidant activity of methanol extracts of five

Table 2: TPC, TFC and Antioxidant activities of different parts of *M. annua*

Plant parts	TPC (µg/mL GAE)	TFC (µg/mL RE)	DPPH (IC_{50} µg/mL)	ABTS (IC_{50} µg/mL)	FRAP (µM Fe^{2+}/g)
Leaves	226.84	152.02	95.97	116.9	404
Stem	56.79	21.78	308.5	217.7	284
Fruit	57.67	51.58	207.8	204.9	309
Flower	149.31	122.22	114.5	142.7	368
Root	72.65	70.35	166.7	158.7	332

Table 3: ANOVA mean squares values of plant parts by DPPH, ABTS and FRAP antioxidant methods

SOV	DF	Leaves	Stem	Fruit	Flower	Root
Treatment	2	100364**	50880.3**	60281.9**	80841.7**	66273.1**
Error	6	0.4688	1.1	0.5	0.1	0.3
Total	8					

*= P < 0.05, ** = P < 0.01

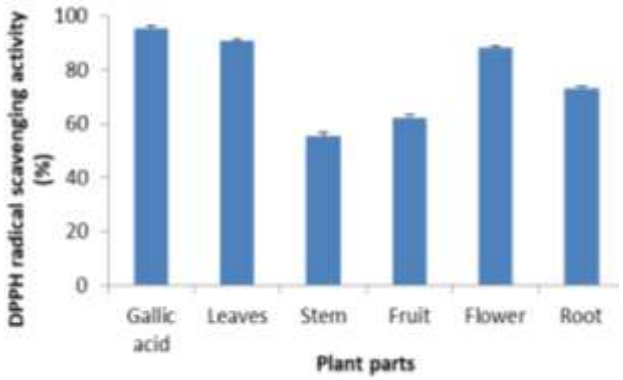

Fig. 3: DPPH antioxidant activity of *M. annua* parts. Results are presented as means of three measurements with standard deviations

different parts of *M. annua* was expressed in terms of % age inhibition (Fig. 3) and IC_{50} values (Table 2). The results were compared with Gallic acid.

Leaves have remarkably higher antioxidant activity with reference compound gallic acid. Flowers and roots also have good antioxidant activity with lower IC_{50} value (114 µg/mL) and (166 µg/mL) respectively. *M. annua* stem revealed lower activity as compared to other parts *i.e.*, (308 µg/mL). Results were reported as mean ± SD of triplicates measurements. The analysis of variance (Table 3) revealed significant differences among plant parts *i.e.*, $P< 0.05$.

ABTS Scavenging Activity

M. annua extracts showed strong to good antioxidant activity in different parts. Percentage inhibition was higher in leaves and flowers extracts comparable to reference sample (Fig. 4). Flowers exhibited promising antioxidant activity (IC_{50} 142 µg/mL) after leaves (Table 2), which has not been reported previously. This supports the arguments that leaves and flowers extracts have greater

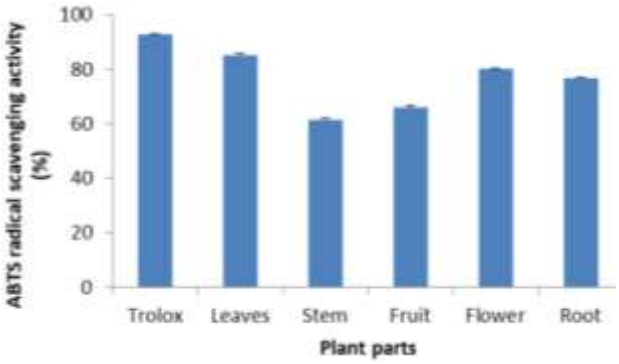

Fig. 4: ABTS antioxidant activity of *M. annua* parts. Results are presented as means of three measurements with standard deviations

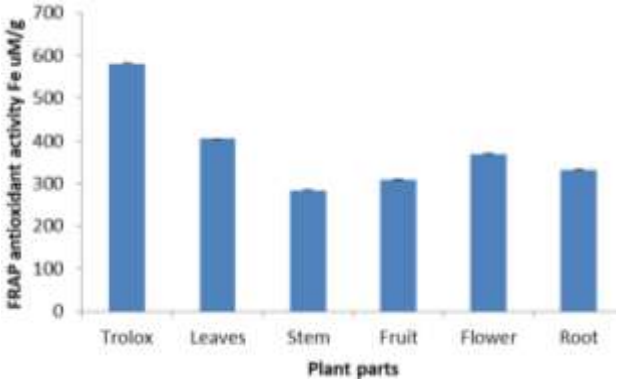

Fig. 5: FRAP antioxidant activity of *M. annua* parts. Results are presented as means of three measurements with standard deviations

phenolic and flavonoid contents compared to other parts. Stem showed lower activity with higher IC_{50} value (217 µg/mL). Means of all parts were significantly differ with each other's *i.e.*, $P< 0.05$ (Table 3).

FRAP Reducing Assay

FRAP reducing power was expressed in µM Fe^{2+}/g of different extracts compared to standard compound (Fig. 5). The FRAP values of leaves and flowers extracts showed good reducing values *i.e.*, leaves (404 µM Fe^{2+}/g) and flowers (368 µM Fe^{2+}/g) respectively as compared to Trolox (580 µM Fe^{2+}/g) (Table 2). The means squares values indicate significant difference among plant parts (Table 3).

Discussion

The results discussed above revealed that, this species is a rich source of mixed hydrophilic phenolic acids and flavonoids with the variety of structural variations *i.e.*, di-, tri- and tetra-glycosides. HPLC-DAD-ESI-MS fingerprinting was found to be suitable and sensitive

technique to identify such polar and thermally labile flavonoid glycosides in this plant.

The MS interpretation enabled us to find the hydroxylation, methylation, acylation and degree of glycosylation (Mabry *et al*., 1970; Markham, 1982; Domon and Costello, 1988; Harborne, 1988).

The identified compounds shared the –*O*-glycosidic class. Methylated and acylated flavonoid glycosides have been characterized first time in this species. Quercetin derivatives were only flavonol glycosides found in this species. The identified compounds are widely distributed in plants as a free aglycone and to somehow in di-glycosidic form (Plazonić *et al*., 2009). The present investigation revealed the tri- and tetra-glycosides with unique hydroxylation, acylation and the sequence/position of glycosylation to the aglycones, which have never been identified in this species/genus and found lesser in literature reports.

A number of identified compounds have previously been shown to have medicinal properties which may contribute to the medicinal effects reported for the consumption of *M. annua*. Apigenin and their glycosides have been shown to have potent antibacterial effects (Hanumantappa *et al*., 2014) and antileukemic activities (Budhraja *et al*., 2012). Apigenin-7-*O*-glucuronide is known to have anti-inflammatory activity (Hu *et al*., 2016). Hispidulin and their glycosides have been reported as effective anticancer agents and the strongest ligand of the benzodiazepine (BZD) site of the GABAA receptor (Kavvadias *et al*., 2004). Luteolin, quercetin and their glycosides have potent antioxidant, antimicrobial, and anticancer activities. Luteolin glycosides revealed strong antioxidant, anticancer and anti-inflammatory activities (Odontuya *et al*., 2005).

Phenolic compounds have been considered powerful *in vitro* antioxidant and proved to be more potent antioxidant than vitamin C and E and carotenoids (Rice-Evans *et al*., 1995). Plant extracts showed strong to good antioxidant activity in different parts of *M. annua*. Leaves revealed higher antioxidant activity by all the methods and comparable to reference compounds. Percentage inhibition was also higher in flowers and root extracts after leaves that support the arguments that these extracts have greater phenolic and flavonoid contents. The analysis of variance depicted that statistical significant difference existed among different methods used. This species possesses good antioxidant activity and this capability can be correlated to different phenolic acids and flavonoid compounds identified in this plant.

Flavonoids have ideal structure activity chemistry for free radical scavenging. The prominent structural features responsible for antioxidant activity are substitution pattern, structure/numbers of –OH groups, 3′,4′ ortho dihydroxy pattern of B ring and 4-carbonyl group in C ring, a catechol like structure of 3- and 5-OH groups in ring C are crucial for scavenging properties of flavonoids. In addition, the scavenging potential enhanced by delocalization of electrons between C_2-C_3 bond and 4-keto arrangement (Wojdyło *et al*., 2007; Procházková *et al*., 2011).

Conclusion

This study provided a more and complete description of phenolic constituents and antioxidant potential of *M. annua* and adds a new and original contribution in the existing literature. It is indicated that this plant can be considered as a rich source of bioactive phenolic constituents and high diversity found in this species implies their potential beneficial effects for human health. So, more studies should be conducted to quantify these entire constituent's for further clinical and biological studies.

Acknowledgements

The first author thanks to Higher Education Commission of Pakistan for providing financial aid regarding Indigenous Scholarship (PhD Fellowship for 5000 scholars Phase II).

References

Arnao, M.B., A. Cano and M. Acosta, 2001. The hydrophilic and lipophilic contribution to total antioxidant activity. *Food Chem*., 73: 239-244

Babu, H.B., L.S. Mohana and A.K. Saravana, 2010. Studies on phytochemical and anticonvulsant property of *Martynia annua* Linn. *Int. J. Phytopharm*., 1: 82–86

Benzie, I.F.F. and J.J. Strain, 1996. The ferric reducing ability of plasma (FRAP) as a measure of "antioxidant power": the FRAP assay. *Anal. Biochem*., 239: 70–76

Brand-Williams, W., M.E. Cuvelier and C. Berset, 1995. Use of free radical method to evaluate antioxidant activity. *Lebensm Wiss U Technol*., 28: 25–30

Budhraja, A., G. Ning, Z. Zhuo, S. Young-Ok, C. Senping, W. Xin, D. Songze, H. Andrew, C. Gang, L. Jia and S. Xianglin, 2012. Apigenin induces apoptosis in human leukemia cells and exhibits anti-leukemic activity in vivo. *Mol. Cancer Ther*., 11: 132–142

Chang, C., M. Yang, H. Wen and J. Chern, 2002. Estimation of total flavonoid content in propolis by two complementary colorimetric methods. *J. Food Drug Anal*., 10: 178–182

Ciesla, L., 2012. Biological fingerprinting of herbal samples by means of liquid chromatography. *Chromatogr. Res. Int*., 2012: Article ID 532418

Dhingra, A.K., B. Chopra and S.K. Mittal, 2013. *Martynia annua* L.: A review on its Ethnobotany, Phytochemical and Pharmacological Profile. *J. Pharmacog. Phytochem*., 1: 135–140

Domon, B.C. and E. Costello, 1988. A systematic nomenclature for carbohydrate fragmentations in FABMS/ MS spectra of glycoconjugates. *Glycoconj. J*., 5: 397–409

Flora, G., M.M. Josephine, M. Chandra, M. Nanthini, K. Shalini, P. Shantha, A.R. Sivam and S. Valli, 2013. Study on Antioxidant potential of different parts of *Martynia annua* Linn. – A road side weed. *Int. J. Dev. Res*., 3: 51–54

Hanumantappa, B., Nayaka, L. Ramesh, Londonkar, K. Madire, Umesh and T. Asha, 2014. Antibacterial attributes of apigenin, isolated from *Portulaca oleracea* L. *Int. J. Bacteriol*., Article ID 175851

Harborne, J.B., 1988. Phytochemical Methods. Chapman and Hall, London

Hu, W., X. Wang, L. Wu, T. Shen, L. Ji, X. Zhao, C.L. Si, Y. Jiang and G. Wang, 2016. Apigenin-7-O-β-D-glucuronide inhibits LPS-induced inflammation through the inactivation of AP-1 and MAPK signaling pathways in RAW 264.7 macrophages and protects mice against endotoxin shock. *Food Funct*., 7: 1002–1013

Kavvadias, D., P. Sand, K.A. Youdim, M.Z. Qaiser, C. Rice-Evans, R. Baur, E. Sigel, W.D. Rausch, P. Riederer and P. Schreier, 2004. The flavone hispidulin, a benzodiazepine receptor ligand with positive allosteric properties, traverses the blood-brain barrier and exhibits anticonvulsive effects. *Brit. J. Pharmacol*., 142: 811–820

Lodhi, S. and A. K. Singhai, 2013. Wound healing effect of flavonoid rich fraction and luteolin isolated from *Martynia annua* Linn. on streptozotocin induced diabetic rats. *Asian Pac. J. Trop. Biomed*., 1: 253–259

Mabry, T.J., K.R. Markham and M.B. Thomas, 1970. *The* Ultraviolet spectra of flavones and flavonols, isoflavones, dihydroxyflavonols. In: *The Systematics Identification of Flavonoids*; Springer–Verlag: New York, USA

Mali, P.C., A.S. Ansari and M. Chaturedi, 2002. Antifertility effect of chronically administered *Martynia annua* root extract on male rats. *J. Ethnopharmacol*., 82: 61–67

Markham, K.R., 1982. *Techniques of Flavonoid Identification*, pp: 36-51. Academic Press: New York, USA

Nagda, D., A. Saluja and C. Nagda, 2009. Antioxidant Activities of Methanolic and Aqueous Extract from Leaves of *Martynia annua* Linn. *Pharmacog. J*., 1: 288–297

Odontuya, G., J.R. Hoult and P.J. Houghton, 2005. Structure-activity relationship for antiinflammatory effect of luteolin and its derived glycosides. *Phytother. Res*., 19: 782–786

Parvati, A. and I.L. Narayana, 1978. Chemotaxonomy of a few taxa of Pedaliaceae. *Curr. Sci*., 47: 282

Pillai, T.S.K., P.P. Thampi and K.C. Verma, 1964. Preliminary pharmacognostiol study of *Martynia diandiae Glox. Madhy. Bhar. J*., 29: 11–13

Plazonić, A., F. Bucar, Ž. Maleš, A. Mornar, B. Nigović and N. Kujundžić, 2009. Identification and Quantification of flavonoids and phenolic acids in burr parsley (*Caucalis platycarpos* L.), using high-performance liquid chromatography with diode array detection and electrospray ionization mass spectrometry. *Molecules*, 14: 2466–2490

Procházková, D., I. Boušová and N. Wilhelmová, 2011. Antioxidant and prooxidant properties of flavonoids. *Fitoterapia*, 82: 513–523

Quirantes, R.P., L. Funes, V. Micol, C.A. Segura and G.A. Fernández, 2009. High performance liquid chromatography with diode array detection coupled to electrospray time-of-flight and ion-trap tandem mass spectrometry to identify phenolic compounds from a lemon verbena extract. *J. Chromatogr. A*., 28: 5391–5397

Rice-Evans, C.A., N.J. Miller, P.G. Bolwell, P.M. Bramley, and J.B. Pridham, 1995. The relative antioxidant activities of plant-derived polyphenolic flavonoids. *Free Rad. Res*., 22: 375–383

Santos-Buelga, C. and G. Williamson, 2003. Methods in polyphenol analysis. The Royal Society of Chemistry, Cambridge; 668

Satyavati, G.V., A.K. Gupta and N. Tandon, 1987. *Medicinal Plants of India*, Vol. 2, pp: 223-229. Indian Council Med. Res. New Delhi, India

Scalbert, A., C. Manach, C. Morand, C. Rémésy and L. Jiménez, 2005. Dietary polyphenols and the prevention of diseases. *Crit. Rev. Food Sci. Nutr*., 45: 287–306

Singleton, V.L., R. Orthofer and R.M. Lamuela-Raventos, 1999. Analysis of total phenols and other oxidation substrates and antioxidants by means of Folin-Ciocalteu reagent. *Methods Enzymol*., 299: 152–178

Su, X., L. Kong, X. Lei, L. Hu, M. Ye and H. Zou, 2007. Biological fingerprinting analysis of traditional Chinese medicines with targeting ADME/Tox property for screening of bioactive compounds by chromatographic and MS methods. *Minirev. Med. Chem*., 7: 87–98

Watt, G., 1972. *Dictionary of the Economic Products of India*, Vol. 5, p: 676. Cosmo Publications: New Delhi, India

Wojdyło, A., J. Oszmianski and R. Czemerys, 2007. Antioxidant activity and phenolic compounds in 32 selected herbs. *Food Chem*., 105: 940–949

Yu, F., L. Kong, H. Zou and X. Lei, 2010. Progress on the screening and analysis of bioactive compounds in traditional Chinese medicines by biological fingerprinting analysis. *Comb. Chem. High Throughput Screen*., 13: 855–868

(Received 05 June 2017; Accepted 02 October 2017)